Chemical Engineering Journal 145 (2008) 185–195

Contents lists available at ScienceDirect

Chemical Engineering Journal

journal homepage: www.elsevier.com/locate/cej

Selective adsorption of gold from complex mixtures using mesoporous adsorbents

Koon Fung Lam[a,b], Chi Mei Fong[a], King Lun Yeung[a,*], Gordon Mckay[a]

[a] Department of Chemical Engineering, Hong Kong University of Science and Technology, Clear Water Bay, KowloonHong Kong, China
[b] Environmental Engineering Program, Hong Kong University of Science and Technology, Clear Water Bay, Kowloon, Hong Kong, China

ARTICLE INFO

Article history:
Received 18 April 2007
Received in revised form 25 March 2008
Accepted 30 March 2008

Keywords:
MCM-41
Separation
Wastewater
Adsorption
Modeling
E-waste

ABSTRACT

Selective gold adsorption was investigated for the NH_2-MCM-41 and SH-MCM-41 adsorbents prepared by grafting aminopropyl and thiolpropyl groups on the surface of the MCM-41 mesoporous silica. The single component adsorption of gold, copper and nickel from salt solutions, and the binary adsorption studies of Au^{3+}/Cu^{2+} and Au^{3+}/Ni^{2+} solutions were carried out for the two adsorbents. Gold adsorption from simulated gold mining solution and gold electroplating wastewater were also reported. The NH_2-MCM-41 and SH-MCM-41 displayed strong affinity for gold in the solution and both exhibited 100% selectivity for the gold in the binary Au^{3+}/Cu^{2+} and Au^{3+}/Ni^{2+} solutions. The NH_2-MCM-41 is more suitable for the gold mining solution, while SH-MCM-41 is efficient for gold adsorption from the electroplating waste containing high amount of organics. The gold was recovered as high purity salt solution by elution with mineral acid for NH_2-MCM-41 and thiolsulfate for SH-MCM-41. The regenerated adsorbent remained selective to gold and exhibited the same adsorption capacity as the fresh adsorbent. Also, the regenerated adsorbent performed well even after several reuses.

1. Introduction

There is a strong economic motivation for the removal and recovery of precious metals from wastes for recycle and reuse, as shown by the recent rise in the price of precious metals driven by strong demand and increasing scarcity. Also, new and emerging applications in energy [1–4], electronics [5], health [6] and environment [7,8] are expected to fuel further demands for gold, palladium and platinum in the coming years. This gives a compelling reason for developing more efficient and environmental-friendly methods for their extraction and recovery from mineral ores and waste materials (e.g., e-wastes, industrial effluents). Indeed, a typical e-waste contains precious (e.g., Au and Ag) along with common (e.g., Cu, Fe) and toxic metals (e.g., Ni, Cd) [9]. Trace amounts of precious metals are also to be found in wastewaters from mining, electronics and electroplating industries [10].

Hydrometallurgical processing remains the standard method for metal extraction from ores [11] and is becoming more popular in many metal recycling processes [12]. The dissolved precious metals (e.g., Ag, Au, Pd, Pt) are often recovered by either adsorption or solvent extraction. The solvent extraction process was originally developed for the uranium mining industry, but also proved to be effective for separating Au(III) ions from solutions containing Pd(II) and Pt(IV) ions [13]. However, adsorption remained popular because of its low cost, easy operation, simple maintenance and large capacity [14]. Activated carbon is used to recover precious gold and interdict mercury in process water from mining operations [15]. However, the nonselective adsorption of metal species makes their recovery for reuse difficult and expensive. This had spurred research into selective adsorption with the goal of developing low cost adsorbents capable of efficient removal, separation and recovery of metals from solutions. These include functionalized silica gels and clays [16,17], ion-exchange resins [18] and bioadsorbents such as chitosans [19].

The use of mesoporous adsorbents for selective adsorption had grown following the report of selective mercury adsorption using thiolated MCM-41 by Feng et al. [20]. Several thiolated mesoporous silicas including SBA-15 and MCM-48 were also shown to be selective for mercury adsorption [21,22]. Brown et al. [23] used the thiolated mesoporous silica to separate mercury from a metal solution containing Hg^{2+}, Cd^{2+}, Pb^{2+}, Zn^{2+}, Co^{2+}, Fe^{3+}, Cu^{2+} and Ni^{2+}. SBA-15 grafted with imidazole-containing chemical groups were reported to be highly selective for Pt^{2+} and Pd^{2+} ions and can separate these precious metals from solutions that also contain Ni^{2+}, Cu^{2+} and Cd^{2+} [24]. Our group had reported the use of mesoporous adsorbents based on MCM-41 for selective adsorption, separation and recovery of precious metal ions including silver [25]

* Corresponding author. Tel.: +852 2358 7123; fax: +852 2358 0054.
E-mail address: kekyeung@ust.hk (K.L. Yeung).

1385-8947/$ – see front matter © 2008 Elsevier B.V. All rights reserved.
doi:10.1016/j.cej.2008.03.019

and gold [26] from solutions containing base metal ions (i.e., Cu^{2+}, Ni^{2+}). Selective mesoporous adsorbents had also been successfully designed for metal separation, removal and recovery from binary mixtures of $Cr_2O_7^{2-}$ and Cu^{2+} [27], Ni^{2+} and Cd^{2+} [28] and Cu^{2+} and Pb^{2+} [29].

This work investigates two mesoporous adsorbents, NH_2-MCM-41 and SH-MCM-41 for selective gold adsorption from complex mixtures. This included a simulated gold mining solution prepared according to the composition provided by Colwyn van der Linde of Invid Technologies and a spent gold electroplating waste provided by a local Hong Kong electroplating company. The adsorption separation (i.e., capacity and selectivity) was analyzed in relation to the physicochemical and adsorption properties of the mesoporous adsorbents. Gold recovery and adsorbent regeneration were also studied.

2. Experimental

2.1. Adsorbent preparation and characterization

The mesoporous MCM-41 silica was prepared at room temperature from an alkaline synthesis solution with a molar composition of 6.6 SiO_2:CTABr:292 NH_4OH:2773 H_2O according to the procedure described in a previous work [26]. The reagents used in the synthesis included tetraethyl orthosilicate (TEOS, 98%), cetyltrimethylammonium bromide (CTABr, 99.3%) and ammonium hydroxide (NH_4OH, 28–30 wt.%) purchased from Aldrich and Fisher Scientific. The MCM-41 was filtered, washed and dried before calcining in air at 823 K for 24 h (i.e., heating rate = 5 K/min) to remove the CTA^+ organic template molecules. The resulting free flowing powder displays little tendency to agglomerate. About 40 g of MCM-41 were prepared for this study.

The NH_2-MCM-41(b) and SH-MCM-41(a) adsorbents were prepared by grafting aminopropyls (i.e., $C_3H_7NH_2$) and thiolpropyls (i.e., C_3H_7SH) on the walls of MCM-41 by an 18 h reflux in dry toluene (>99.5%, Mallinckrodt) solutions containing 0.1 mol of 3-aminopropyl-trimethoxysilane (APTS, 97%, Aldrich) and (3-mercaptopropyl) triethoxysilane (MPTS, 95%, Fluka), respectively [25,26,30]. NH_2-MCM-41(a) was prepared by reflux from a solution containing 0.003 mol of APTS to give an aminopropyl loading of 1.0 mmol/g. The mesoporous adsorbents were filtered, washed with toluene and dried overnight in an oven at 383 K. The prepared MCM-41 and mesoporous adsorbents were characterized by X-ray diffraction (XRD, Philips 1830), N_2 physisorption (Coulter SA 3100), Fourier transform infrared spectroscopy (FTIR, PerkinElmer GX 2000), X-ray photoelectron spectroscopy (XPS, Physical Electronics PHI 5000) and elemental analysis (EA, Elementar Vario EL III) to determine their physical and chemical properties. The particle size distribution and surface Zeta potential were measured using Coulter Beckman Zeta-potential analyzer.

2.2. Single and binary components adsorptions

The single and binary component adsorptions of gold, copper and nickel were measured using 0.1 g of adsorbent for 100 ml aqueous solutions of gold(III) chloride (99%, Aldrich), copper(II) chloride (98%, Aldrich) and nickel(II) nitrate hexahydrate (99%, Aldrich). The pH was adjusted to 2.5 ± 0.02 by adding small amount of hydrochloric acid. The batch adsorption experiments were conducted in a shaker bath kept at a constant temperature of 295 ± 2 K. The equilibrium adsorption was measured at the end of five days experiment. The samples were filtered to remove and recover the adsorbent, and the metal concentrations analyzed by inductively coupled plasma, atomic emission spectrometer (ICP-AES, PerkinElmer Optima 3000XL). Three measurements were made for each sample and the results were averaged. The instrument was calibrated with 5, 10 and 20 ppm standard solutions before each set of measurements. The ICP standard solutions of 1000 ppm Au (99.999%) in 2% HCl, 1000 ppm Cu (99.999%) in 2% HNO_3 and 1000 ppm Ni (99.99%) in 2% HNO_3 were purchased from High-Purity Standards. The equilibrium adsorption capacity was calculated from Eq. (1).

$$q_{e,i} = \frac{(C_o - C_e)_i V}{m} \quad (1)$$

where $q_{e,i}$ (mmol/g) is the adsorption capacity, $C_{o,i}$ (mM) and $C_{e,i}$ (mM) are the initial and final concentrations of metal ion i, respectively. V (L) is the solution volume and m (g) is the mass of adsorbent used for the adsorption. The single component adsorption data was described by the Freundlich adsorption equation shown in Eq. (2), and the LeVan and Vermeulen equation (i.e., Eq. (3)) was used to predict the binary adsorptions from the single component adsorption data [31].

$$q_{cal,i} = K_f C_{e,i}^n \quad (2)$$

where $q_{cal,i}$ is the calculated adsorption capacity of component i. K_f and n are the Freundlich parameters. $C_{e,i}$ is the concentration of component i after the adsorption.

$$q_{e,1} = \frac{n(K_1/n_1)^{1/n_1} C_{e,1}}{[(K_1/n_1)^{1/n_1} C_{e,1} + (K_2/n_2)^{1/n_2} C_{e,2}]^{1-n_1}} \quad (3)$$

where $q_{e,1}$ is the amount of component 1 adsorbed at equilibrium, $C_{e,1}$ and $C_{e,2}$ are the equilibrium concentrations of components 1 and 2, respectively, and K_1, K_2 are the values of Freundlich constants from the single component adsorption isotherms of components 1 and 2, respectively.

2.3. Gold adsorption from complex mixtures

The NH_2-MCM-41 and SH-MCM-41 adsorbents were tested for gold adsorption and separation from two complex mixtures. The composition of the simulated gold mining solution was from an actual, large scale gold refinery employing Miller chlorination process for casting impure gold into anode plates. The solution contained 84 ppm Au, 33 ppm Pd, 33 ppm Cu, 33 ppm Fe and 0.04 ppm Pt and was prepared from the metal chloride salts of gold ($AuCl_3$, 99%, International Lab), palladium ($PdCl_2$, 99%, Aldrich), platinum (H_2PtCl_6, Aldrich), copper and iron ($FeCl_3$, 99%, Aldrich). The pH of the solution was adjusted to 2.5 by adding a dilute HCl solution.

A batch of spent gold electroplating waste was collected on-site, before the wastewater treatment process. The sample was refrigerated (i.e., 283 K) and stored in the dark. Three milliliters of the electroplating waste was microwave digested in 10 ml aqua regia solution (3 HCl:1 HNO_3) for 1 h before analysis by ICP-AES to obtain the metal composition. The chemical oxygen demand (COD) and the total organic content (TOC) were measured using Hach COD reactor with DR/2400 detector and Shimadzu TOC-5000A, respectively. Measurements were made on the undiluted and diluted (50×) wastewater. Two milliliters of sample solution was added to standard COD reagent containing potassium dichromate and mercuric sulfate. The mixture was allowed to react in a 423 K reactor for 2 h, before colorimetric analysis. TOC is obtained indirectly by measuring the total carbon obtained by the total combustion of the organics in the sample over a catalyst bed at 953 K and inorganic carbon (i.e., carbonates) by phosphoric acid reaction. The carbon dioxide produced by the reactions was measured by a non-dispersive infrared detector and used

Table 1
Physical and chemical properties of the mesoporous silica adsorbents

	Surface area (m^2/g)	Pore size[a] (nm)	Moiety	FTIR signals (cm^{-1})	Loading of functional groups[b] (mmol/g)	Adsorption capacity at pH 2.5 (mg/g (mmol/g))		
						Au^{3+}	Cu^{2+}	Ni^{2+}
MCM-41	1070	3.09	OH	3757 (O—H)	–	0	0	0
NH_2-MCM-41a	772	2.82	NH_2	3360 and 3288 (N—H), 1600 (C—N)	1.01	78 (0.40)	0	0
NH_2-MCM-41b	774	2.92	NH_2		2.26	275 (1.40)	0	0
SH-MCM-41	990	3.02	SH	2577 (S—H)	1.00	195 (0.99)	0	0

[a] Pore size was calculated based on d-spacing measured by XRD, BET surface area and pore volume by nitrogen physisorption [32].
[b] Amount was calculated from elemental analysis and thermogravimetric experiment.

to calculate the total and inorganic carbon content of the sample. A detailed chemical analysis of the organic components in the mixture was not carried out per request by the company because of proprietary issue. The raw waste solution was used for adsorption *without* pH adjustment. Part of the sample was treated with ozone ($100\,g\,O_3\,m^{-3}$) produced from high purity oxygen gas by an electrical discharge ozone generator (Trailigaz, Ozoconcept OZC100).

3. Results

3.1. MCM-41 and mesoporous adsorbents

The detailed description of the mesoporous MCM-41 silica and its derived NH_2-MCM-41 and SH-MCM-41 was published elsewhere [25,26,30]. Table 1 lists the physical, chemical and adsorption properties of the three mesoporous materials. The disc-shaped MCM-41 had a narrow particle size distribution with a mean particle diameter of $0.75 \pm 0.15\,\mu m$ and a thickness of $0.10 \pm 0.03\,\mu m$ according to electron microscopy and light scattering measurements. The MCM-41 had a calculated pore size of 3.09 nm and a BET surface area of $1070\,m^2\,g^{-1}$. XPS detected only silicon and oxygen from the calcined MCM-41 with a trace amount of carbon from the adsorbed ambient organics. The FTIR detected signals belonging to the surface silanol groups at $3675\,cm^{-1}$, the Si—O—Si bridges between 1000 and $2000\,cm^{-1}$ as well as a broad peak at $3428\,cm^{-1}$ from the adsorbed water molecules. Table 1 summarizes the BET surface area, the average pore diameter and the predominant surface chemical moieties found on the MCM-41.

The particle size and morphology did not change after the aminopropyls and thiolpropyls were attached to the MCM-41, but the surface area and pore size decreased for both NH_2-MCM-41 and SH-MCM-41 as shown in Table 1. Elemental analysis determined that NH_2-MCM-41(a) and NH_2-MCM-41(b) had, respectively, 1.00 and 2.26 mmol/g of grafted aminopropyls, while the SH-MCM-41 had 1.00 mmol/g of thiolpropyls. The XPS analysis of NH_2-MCM-41 measured a C_{1s} binding energy of 285.0 eV that is typical of carbons in the organic alkyl chains and N_{1s} binding energy of around 399.5 eV common to amino compounds. A carbon-to-nitrogen (C/N) ratio of 3.38 was obtained, indicating that about 10% of the methoxy groups in the 3-aminopropyltrimethoxysilane remained unreacted. The samples also displayed infrared signals at 3267 and $3352\,cm^{-1}$ belonging to amine stretching and at 2925 and $2849\,cm^{-1}$ assigned to C–H asymmetric and symmetric bands from *n*-propyl. The XPS data of SH-MCM-41 also displayed C_{1s} binding energy of 285.0 eV from the *n*-propyl and $S_{2p3/2}$ binding energy of 164.0 eV, which is close to the value of 163.8 eV found in many alkylthiol (RSH) molecules [33]. The SH-MCM-41 had infrared signals at $2571\,cm^{-1}$ from S–H stretching in addition to the 2925 and $2849\,cm^{-1}$ bands from *n*-propyl.

3.2. Single and binary components adsorptions

The single component adsorption experiments were conducted at pH 2.5, since the gold solution becomes unstable and precipitates at pH greater than 4. The results showed that MCM-41 does not adsorb gold, copper or nickel ions despite its enormous surface area (Table 1). The NH_2-MCM-41(a) and SH-MCM-41 adsorb gold but not the copper or nickel ions as shown in Fig. 1a and b. The adsorption was fast and equilibrium was reached within 20 min. This indicates that the chemical moieties grafted inside the MCM-41 pores remained readily accessible in spite of the observed decrease in the pore size (Table 1). Fig. 1a plots the equilibrium adsorption isotherms for gold, copper and nickel on NH_2-MCM-41(a). The NH_2-MCM-41(a) adsorbs 0.4 mmol gold per gram adsorbent (i.e., 78.8 mg/g), but not copper or nickel. The adsorption capacity of SH-MCM-41 for gold is 0.99 mmol/g or 195 mg/g. The adsorption data fit Freundlich adsorption model well as shown in the figures. The calculated values for the constant *K* and exponent *n* are 0.80 and 0.11 for the NH_2-MCM-41 and 0.98 and 0.17 for the SH-MCM-41 (cf. Table 2).

The number of RNH_2 group in NH_2-MCM-41(b) was increased to 2.26 mmol/g, in order to obtain a comparable adsorption capacity as the SH-MCM-41 for the binary component adsorption experiments. Fig. 1c and d plots the equilibrium adsorption capacity of NH_2-MCM-41(b) and SH-MCM-41 adsorbents as a function of equilibrium gold concentration in the binary solutions. The experiments were conducted using solutions with equimolar metal ion concentrations at a fixed pH of 2.5 and temperature of $295 \pm 2\,K$. Both adsorbents adsorb only the gold in total exclusion of the copper and nickel ions. This means that NH_2-MCM-41(b) and SH-MCM-41 are 100% selective for gold adsorption under the experimental conditions. The maximum amounts of gold adsorbed by NH_2-MCM-41(b) from the $AuCl_3/CuCl_2$ and $AuCl_3/Ni(NO_3)_2$ solutions are comparable and have the same value of 1.05 mmol/g (200 mg/g), which is slightly less than the single component adsorption capacity (Table 1). The SH-MCM-41 has an adsorption capacity of 0.97 mmol Au/g (191 mg Au/g). Fig. 1c and d shows that the simplified form of LeVan and Vermeulen equation based on the single component Freundlich isotherms fits the binary adsorption data after the effects of anion on dissociation of the metal salts. However, the model does not account for the possibility that anions can compete for adsorption on the protonated aminopropyls in NH_2-MCM-41 and this may explain the larger discrepancy between model and experiment in Fig. 1c. The model parameters are listed in Table 2.

The effects of pH on gold adsorption were investigated and the results are shown in Fig. 2. The surface Zeta potential of the mesoporous adsorbents was measured at different pH and plotted in Fig. 2a. The plots show that NH_2-MCM-41(b) and SH-MCM-41 have point of zero charge (p.z.c.) at pH 3.5 and pH 3.0, respectively. The NH_2-MCM-41(b) is completely protonated at pH less than 2.8 and displays a positively charged surface below the p.z.c. On the

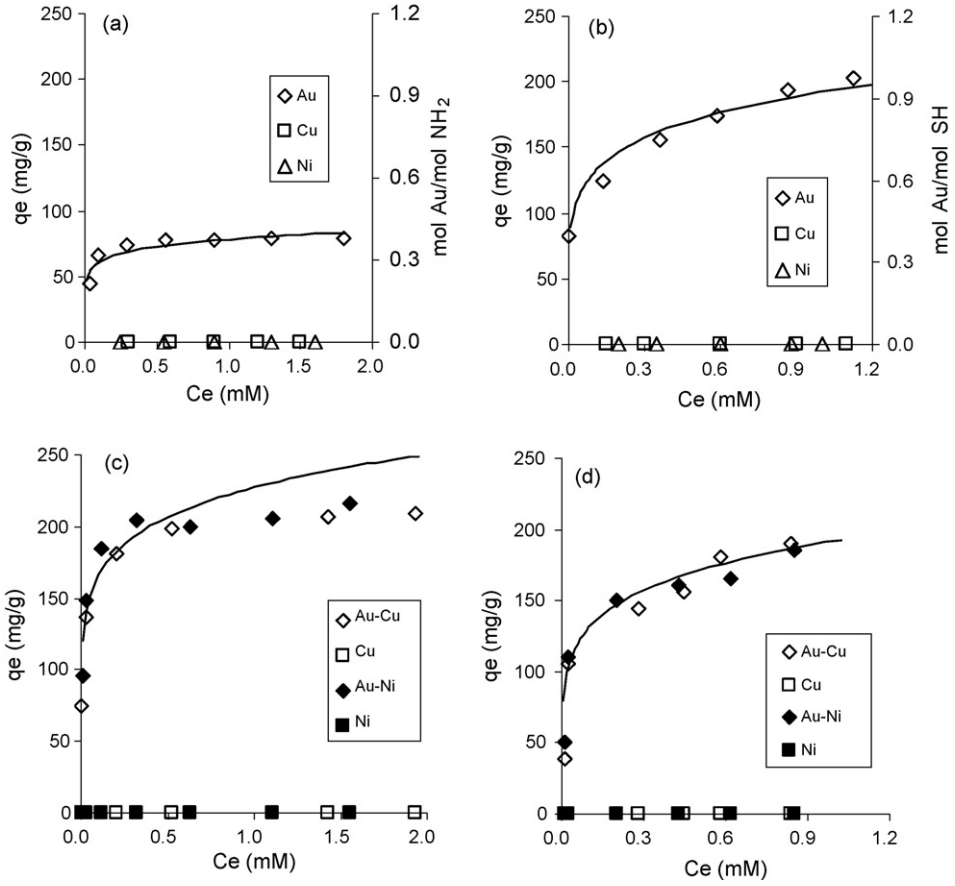

Fig. 1. Single component adsorption of gold, copper and nickel on (a) NH_2-MCM-41(a) and (b) SH-MCM-41 (1 mmol functional group/g adsorbent, 0.1 g adsorbent per 100 ml solution, pH 2.5 and $T = 295 \pm 2$ K). Metal adsorption on (c) NH_2-MCM-41(b) and (d) SH-MCM-41 from Au^{3+}/Cu^{2+} and Au^{3+}/Ni^{2+} binary components solutions (0.1 g adsorbent per 100 ml solution, $[Au^{3+}]/[M^{2+}] = 1$, pH 2.5 and $T = 295 \pm 2$ K). Please note symbols represent experimental data and lines represent model calculation.

other hand, the SH-MCM-41 has a weak surface charge. Fig. 2b shows the presence of Au(III) ions and their adsorption have a considerable effect on the surface Zeta potential of the adsorbents. The data also suggest that the mechanisms of gold adsorption on NH_2-MCM-41 and SH-MCM-41 are different. The Zeta potential plot of NH_2-MCM-41(b) shows a shift in the p.z.c. towards a higher pH value (i.e., pH 4.0 versus pH 3.5) and in addition exhibits a more strongly charged surface. Unlike the original Zeta potential plot in Fig. 2a, the surface of SH-MCM-41 with gold ions displays a strong negative charge over the entire pH range of the study (Fig. 2b).

The gold adsorptions from equimolar $AuCl_3/CuCl_2$ solutions with pH between 2.0 and 4.0 are plotted in Fig. 2c and d. The gold is present as a negatively charged $AuCl_4^-$ anion at these pHs [35]. The results show that copper was not adsorbed at this pH range and gold was the only metal adsorbed by NH_2-MCM-41(b) and SH-MCM-41. One gram of NH_2-MCM-41(b) adsorbed about 206 mg gold and a gram of SH-MCM-41 adsorbed 185 mg gold. These are equivalent to 0.46 Au per RNH_2 and 0.95 Au per RSH on NH_2-MCM-41(b) and SH-MCM-41, respectively. It can be seen in the figures that the LeVan and Vermeulen model accurately predicts the gold adsorption at different pH. Fig. 2d shows that gold adsorption on SH-MCM-41 is unaffected by changes in pH, whereas the gold adsorption on NH_2-MCM-41 displays a decreased value at low pH as shown in Fig. 2c.

3.3. Gold adsorption from complex mixtures

3.3.1. Gold mining solution

The simulated gold mining solution was based on an actual composition from a large scale gold refinery that uses Miller chlorination process for casting impure gold into anode plates followed by the Wohlwill electrolytic process. The solution contains 84 ppm Au, 33 ppm Pd, 33 ppm Cu, 33 ppm Fe and 0.04 ppm Pt metal chloride salts at pH 2.5 (Fig. 3a). Three 100 ml gold mining solutions

Table 2
Parameter values for model calculation

	Equation	Parameter	SH-MCM-41	NH_2-MCM-41
LeVan and Vermeulen equation	$q_{e,1} = \frac{n(K_1/n)^{1/n}C_{e,1}}{[(K_1/n)^{1/n}C_{e,1}+(K_2/n)^{1/n}C_{e,2}]^{1-n}}$	K_{Au}	0.98	0.80
		K_{Cu} or K_{Ni}	0	0
		n	0.17	0.11
Dissociation constant of metal salts [34]	$K_{A_mB_n} = \frac{[A_mB_n]}{[A]^m[B]^n}$	pK_{AuCl_3}	29.6	
		pK_{CuCl_2}	0.1	
		$pK_{Cu(NO_3)_2}$	0	
		pK_{NiCl_2}	0	
		$pK_{Ni(NO_3)_2}$	–	

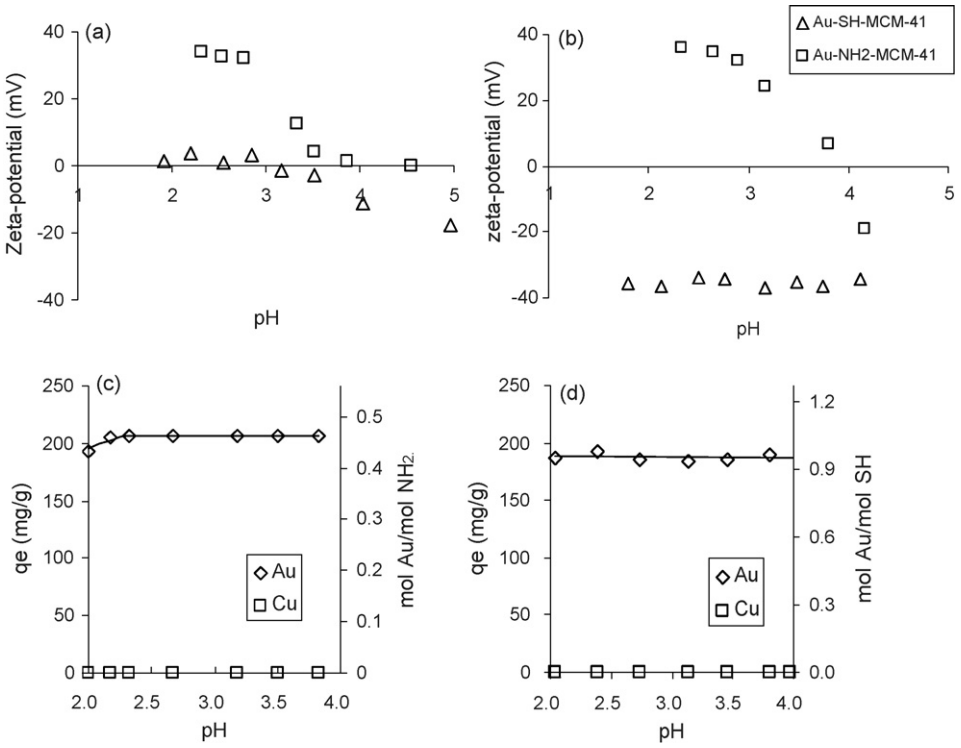

Fig. 2. Effects of pH on the surface Zeta potential of the adsorbents (a) before and (b) after gold adsorption and the Au^{3+}/Cu^{2+} binary components adsorption of (c) NH_2-MCM-41(b) and (d) SH-MCM-41 against pH (0.1 g adsorbent per 100 ml solution, $[Au^{3+}] = [Cu^{2+}] = 1$ mM and $T = 295 \pm 2$ K). Please note symbols represent experimental data and lines represent model calculation.

were prepared and 0.10 g of NH_2-MCM-41(b), SH-MCM-41 and CN-MCM-41 were added to each solution and allowed to equilibrate for 1 h. Fig. 3b–d displays the composition of the solutions after adsorption. It can be seen from Fig. 3b that NH_2-MCM-41(b) adsorbed and removed all the gold and palladium from the solution, but not the copper, iron or platinum. The gold in the solution was also completely adsorbed by SH-MCM-41 as shown in Fig. 3c. However, the adsorbent also adsorbed all the palladium and platinum in the solution as well as small quantities of copper and iron. Cyanide is commonly used to extract gold from ores and CN-MCM-41 containing 1.96 mmol/g propionitrile (i.e., C_2H_4CN) was prepared according to the procedure reported in a previous work [27]. Fig. 3d shows that CN-MCM-41 is a poor adsorbent and the grafted cyano groups have poor affinity for gold adsorption. Fig. 4 summarizes the amount of metals adsorbed from the solution by each adsorbent. The results indicate that NH_2-MCM-41(b) is most selective among the three adsorbents investigated in this study.

Elution is a common method used in the recovery and regeneration of spent adsorbents. Table 3 shows a simple acid wash with 1 M HCl solution recovers 72% of the adsorbed gold, while complete recovery (i.e., 99.9%) was obtained using a 5 M HCl solution. Even neutral saline solution (i.e., 5 M NaCl) was capable of recovering 10% gold from the adsorbents and an acidified saline solution containing 1 M HCl and 4 M NaCl was as effective as 5 M HCl for gold recovery. It is possible to recover high purity gold (> 90%) from the spent NH_2-MCM-41(b) adsorbent by selective elution method. Spent NH_2-MCM-41 with co-adsorbed 0.47 mmol/g Pd and 0.44 mmol/g Au [36] were eluted with different concentrations of HCl. Fig. 5a and b shows that co-adsorbed gold and palladium on NH_2-MCM-41 desorbed at different rates depending on the pH, and Fig. 5c plots the Au/Pd ratio in the eluent. The gold desorbed at a faster rate than palladium, particularly at low acid concentration. Using 0.1 M HCl elution solution, nearly half of the adsorbed gold on NH_2-MCM-41(b) was recovered as 95% pure $AuCl_3$ solution. Elution with concentrated acid recovers more gold but also desorbs more palladium resulting in a lower purity. After the recovery of the high purity gold solution, the adsorbent was eluted a second time in a 5 M HCl to desorb the remaining adsorbed gold and palladium giving a roughly equimolar gold and palladium chloride salts solution. The elution process also regenerated the adsorbent, which can be reused without lost of performance (Table 4).

Table 3
Gold recovery from the spent NH_2-MCM-41(b) and SH-MCM-41 adsorbents

Eluent	Percent recovery	
	NH_2-MCM-41	SH-MCM-41
1 M HCl	72.0	<1.0
5 M HCl	99.9	<1.0
5 M NaCl	≤10.0	<1.0
1 M HCl + 4M NaCl	99.9	<1.0

3.3.2. Gold electroplating waste

The spent electroplating waste had a high TOC content and COD value as shown in Table 5. Besides gold, it contained a large amount of cobalt and trace quantities of chromium, manganese, nickel and zinc. Fig. 6a and b plots the metal adsorptions on NH_2-MCM-41(b) and SH-MCM-41 adsorbents. The adsorptions were carried out using the raw waste solution without pH adjustment to avoid possible solid precipitation. Dilution was used to obtain different solution concentrations. Fig. 6a shows that NH_2-MCM-41(b) adsorbs cobalt more than gold from the waste solution, while on the other hand SH-MCM-41 adsorbs only gold as shown in Fig. 6b. Ozone treatment was used to oxidize and remove much of the organics from raw waste solutions. The treated solution contained less than 2000 ppm TOC compared to 21,000 ppm in the original

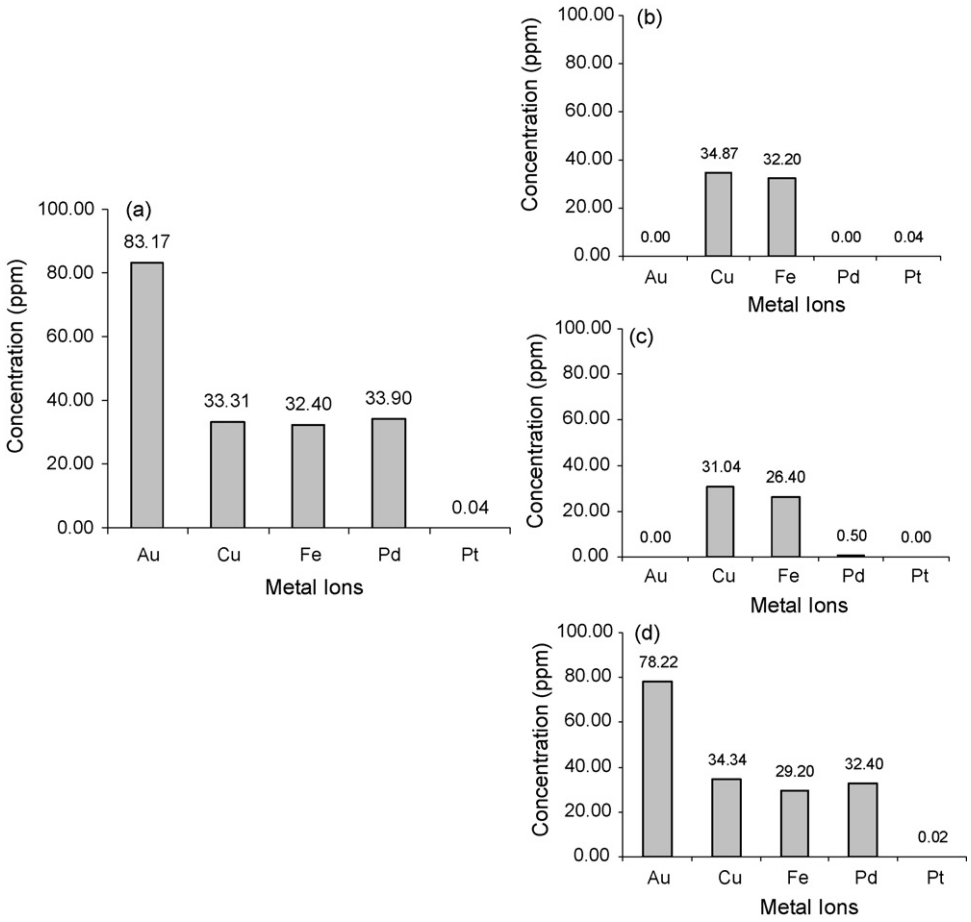

Fig. 3. Compositions of the simulated gold mining solutions (a) before and after adsorption by (b) NH_2-MCM-41(b), (c) SH-MCM-41 and (d) CN-MCM-41 (0.1 g adsorbent per 100 ml solution, pH 2.5 and $T = 295 \pm 2$ K).

wastewater. Fig. 6c shows that the removal of the organics did not significantly improve the selectivity of NH_2-MCM-41(b). Fig. 6d shows that the SH-MCM-41 is insensitive to the organic pollutants in the electroplating wastewater and remained highly selective to gold adsorption.

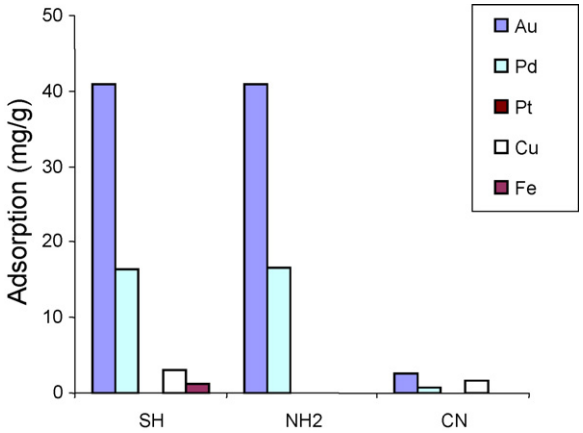

Fig. 4. Metals adsorbed from the simulated gold mining solution per gram of NH_2-MCM-41(b), SH-MCM-41 and CN-MCM-41 adsorbents (0.1 g adsorbent per 100 ml solution, pH 2.5 and $T = 295 \pm 2$ K).

4. Discussion

4.1. Adsorption and separation experiments

Fig. 7 displays the schematic drawings of the grafted organic moieties on NH_2-MCM-41(a), NH_2-MCM-41(b) and SH-MCM-41 according to XPS, FTIR, elemental analysis and TGA/DTA [25,26] data referred to in Table 1. The XPS analysis of NH_2-MCM-41(a) and NH_2-MCM-41(b) gave C/N ratios of 3.62 and 3.38 indicating that not all of the methoxys on the silane group had reacted during the grafting of the aminopropyls on MCM-41 as shown by the illustrations. The XPS data were also independently confirmed by elemental analysis and TGA/DTA experiments. It also shows the interactions between the grafted amino groups and the unreacted surface hydroxyls on NH_2-MCM-41(a) as observed by FTIR [26].

Table 4
Repeated adsorption and regeneration of spent NH_2-MCM-41(b) adsorbents[a]

Run	Adsorption (mg/g)	Gold selectivity (%)	Desorption (mg/g)	Percent regeneration
1	226	100	225	99
2	215	100	212	99
3	212	100	212	100
4	224	100	224	100
5	221	100	217	98

[a] Adsorption was conducted using 0.125 g adsorbent per 100 ml solution, $[Au^{3+}] = [Cu^{2+}] = 3$ mM, pH 2.5 and $T = 295 \pm 2$ K. The gold recovery and adsorbent regeneration uses 3 ml of 5 M HCl at room temperature.

Table 5
Composition of the raw gold electroplating waste solution

pH	COD (mg/l)	TOC (ppm)		Metal	Concentration after digestion (ppm)	R.S.D. (%)
		Dilution for measurement	Actual value			
4.90	57320	50×	22610	Au	5800	1.1
				Cr	37.1	4.0
				Co	1340	0.2
				Mn	0.099	7.5
		500×	20745	Ni	1.21	8.7
				Zn	1.53	3.2

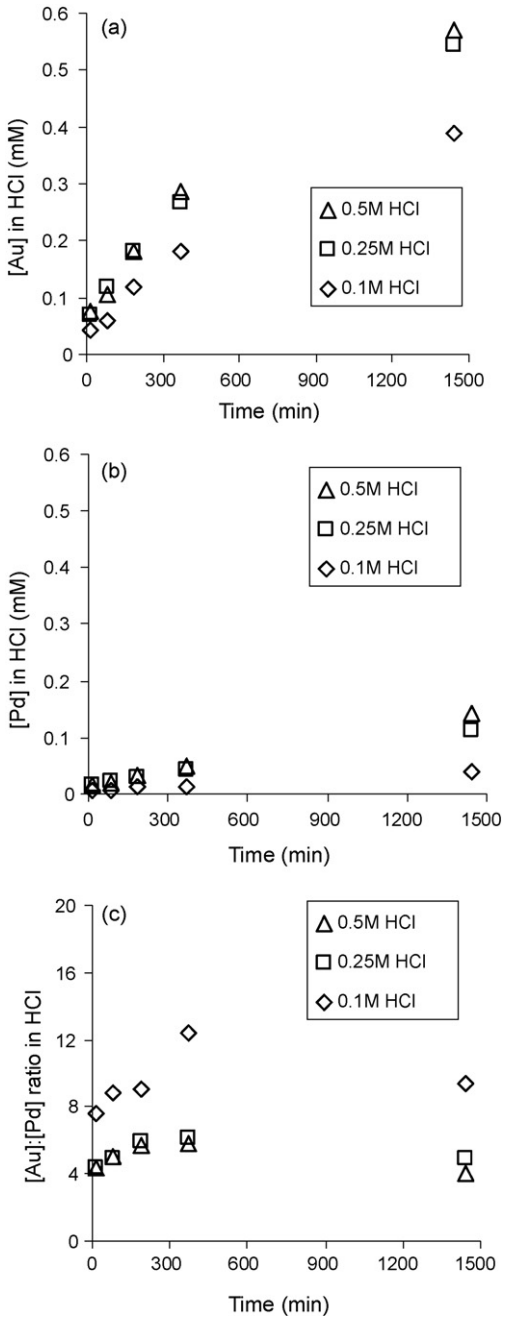

Fig. 5. Desorptions of (a) gold and (b) palladium co-adsorbed on NH_2-MCM-41(b) and (c) the Au/Pd ratio in the wash solution plotted as a function of time and acid eluent concentrations.

The elemental analysis of SH-MCM-41 gave 5C:1S indicating that one of the ethoxides remained intact and unreacted. Therefore, the thiolpropyls on SH-MCM-41 were attached to the pore wall by two Si—O—Si bonds. In spite of the presence of unreacted surface hydroxyls, there was no evidence of interactions with the attached thiolpropyls.

The Pearson's hard-soft, acid-base (HSAB) principle [37] proved useful for predicting metal adsorption on mesoporous adsorbents [25]. The HSAB principle describes the preferential interactions between the Lewis acids and bases of similar "hardness". The grafted aminopropyls on NH_2-MCM-41 acts as a Lewis base at pH above p.z.c. and preferentially adsorbed positively charge metal cations (i.e., Lewis acids) by forming dative bonds. Fig. 2a shows the adsorbents becomes positively charged at pHs below p.z.c. as the aminopropyl groups become protonated. Gold adsorption on NH_2-MCM-41 at low pH is between the protonated amino groups (i.e., $^{+}NH_3$-MCM-41) that are strong Lewis acid and the basic $AuCl_4^-$ anions found at pH below 4 [35]. Fig. 8 shows that the gold ions can adsorb on aminopropyls by either ion exchange (scheme 1) or complexation (scheme 2). Scheme 2 is more consistent with the adsorption data of NH_2-MCM-41(b) where one gold atom was adsorbed for every two aminopropyl groups on the adsorbent (Table 1). It also explains why the NH_2-MCM-41(b) displayed a stronger positive surface charge after adsorbing the negative $AuCl_4^-$ anions (Fig. 2b). The presence of unreacted surface hydroxyls was detected by FTIR on the NH_2-MCM-41(a). Although metal adsorption on the unreacted silanols is not expected to be significant according to the adsorption results for MCM-41 (Table 1), however the interactions between the unreacted silanols and the grafted chemical moieties could affect the metal adsorption. Indeed, NH_2-MCM-41(a) adsorbed 1 Au:2.5 RNH_2 that is less than the expected value of one gold atom for every two aminopropyls.

The "acid" Cu^{2+} and Ni^{2+} cations from the binary adsorption experiments (Fig. 1c) and the Cu^{2+} and Fe^{3+} from the simulated gold mining solutions (Fig. 3b) were repelled by the positively charged, "acidic" protonated aminopropyl groups and were not adsorbed. This explains the excellent selectivity of NH_2-MCM-41 for gold adsorption at low pH (i.e., $<pH_{p.z.c.}$). The adsorptions of electroplating waste solution (Fig. 6a and c) were carried out at pH 4.9 that is above the $pH_{p.z.c.}$ of NH_2-MCM-41. The $-RNH_2$ groups predominate at this pH and the NH_2-MCM-41 adsorbed mainly Co^{2+} (Fig. 6a). The high organic content of the electroplating waste could interfere with the adsorption process as many of the chemicals contains carboxylic, amino and thiol groups that could interact with the grafted aminopropyls. However, the NH_2-MCM-41 still adsorbed Co^{2+} (Fig. 6c) even after removing 90% of the organics by ozone treatment. This suggests that pH is the main factor for the poor gold adsorption from the electroplating waste solution.

Fig. 2a shows that SH-MCM-41 has a weak surface charge and unlike NH_2-MCM-41, the thiolpropyls were not protonated at low pH. Indeed gold adsorption remained unchanged with pH as shown in Fig. 2d. Trokhimchuk et al. [38] proposed several schemes for gold

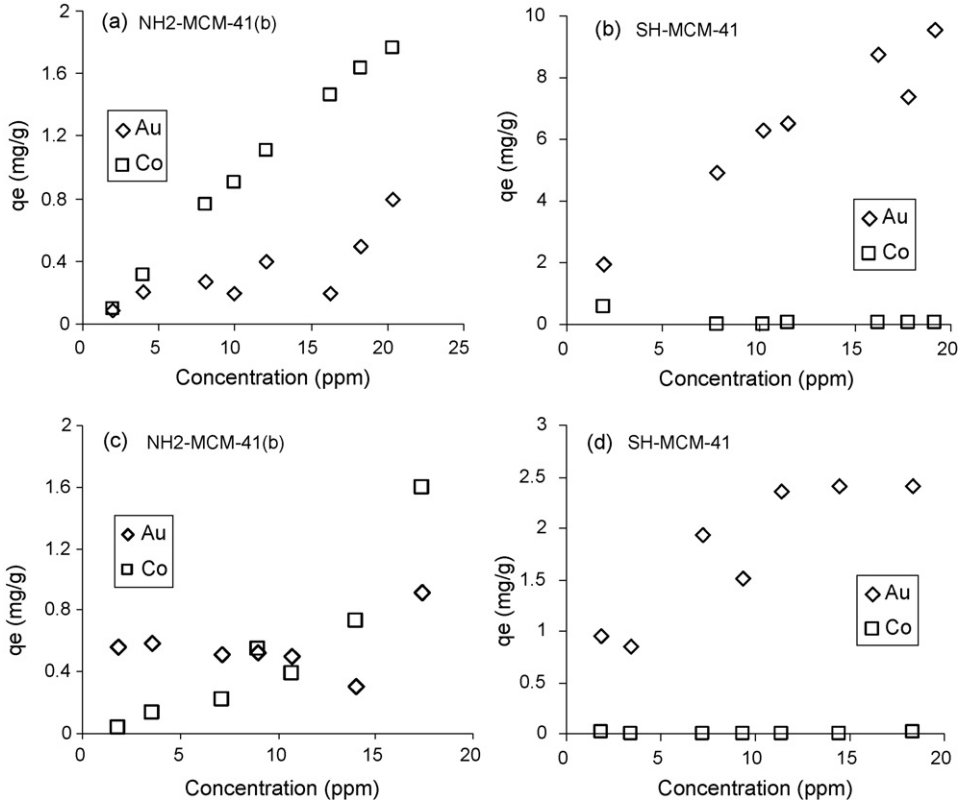

Fig. 6. Metal adsorption from gold electroplating wastewater (a and b) before and (c and d) after organic removal by ozonolysis.

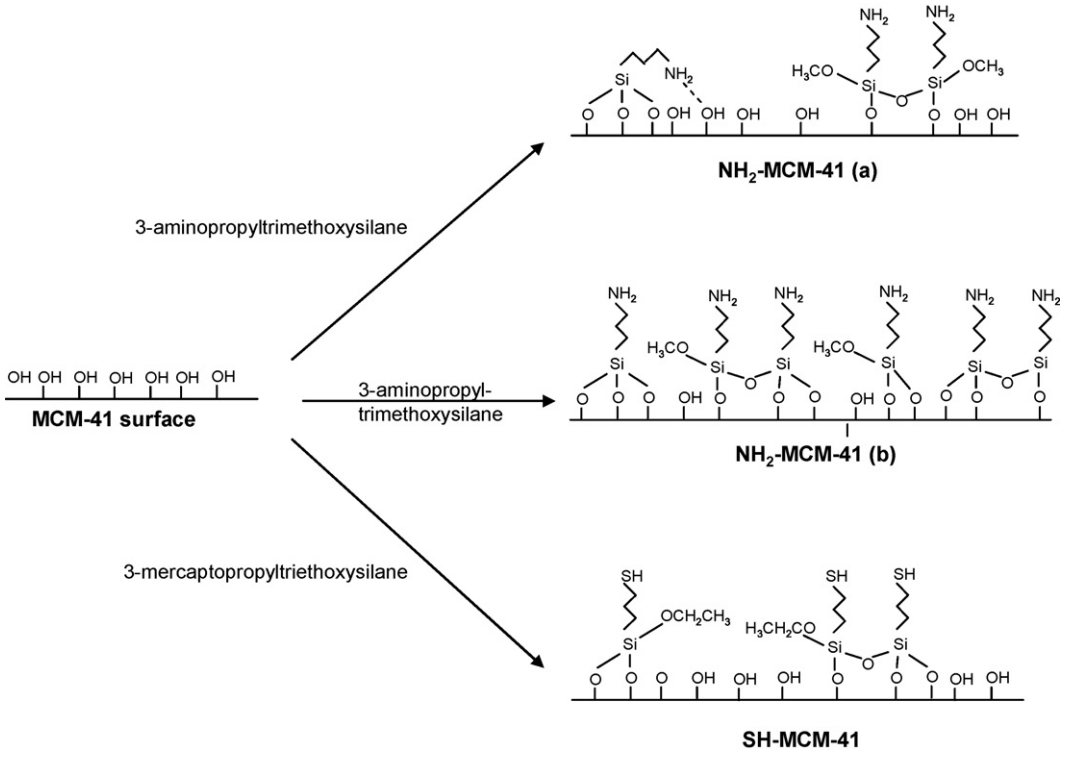

Fig. 7. Schematic drawings of the organic moieties grafted on MCM-41.

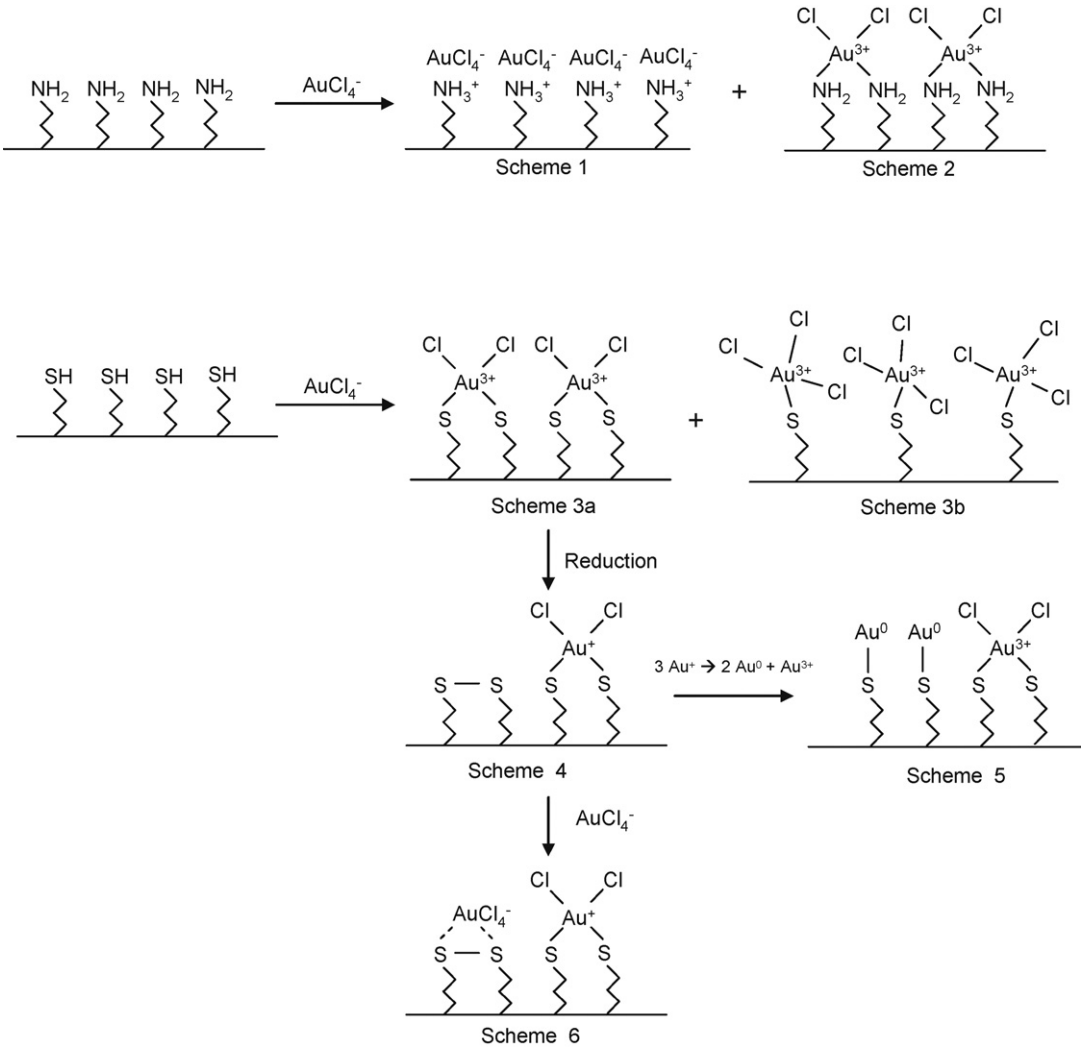

Fig. 8. Schemes for gold adsorption on NH_2-MCM-41 and SH-MCM-41.

adsorption on thiolpropyls and these are illustrated in Fig. 8. Gold can adsorb by forming complex with the thiol groups (schemes 3a and b). It is possible for the adsorbed Au(III) complex to undergo reduction to Au(I) with concomitant oxidation of thiolpropyls to dithiolpropyls as shown in scheme 4. The Au(I) atoms can react and liberate a Au(III) ion and deposit a metallic gold (scheme 5). Gold can also adsorb on the dithiolpropyls according to scheme 6. The gold adsorption on SH-MCM-41 is consistent with scheme 3b, with one gold ion adsorbing on one thiolpropyl group. The gold anion adsorbed according to this scheme (i.e., $-RSAuCl_3^-$) will also give the adsorbent surface a negative charge that is in agreement with the Zeta potential measurement shown in Fig. 2b.

The thiolpropyl group on SH-MCM-41 is known to have good affinity for silver, gold, palladium and platinum. It is considered a soft Lewis base according to HSAB principle and should prefer not to adsorb the hard Lewis acids such as Cu^{2+} and Ni^{2+} used in the binary adsorption experiment, or the Cu^{2+} and Fe^{3+} in the simulated gold mining solution and the Co^{2+} found in the electroplating waste solution. Indeed, the SH-MCM-41 exhibits excellent selectivity for gold adsorption from binary solutions containing Cu^{2+} and Ni^{2+} ions (Fig. 1d). However, SH-MCM-41 adsorbed palladium and platinum along with gold from the simulated mining gold solution (Fig. 3c). Also, the small amounts of Cu^{2+} and Fe^{3+} were most likely removed by precipitation caused by redox reactions during metal adsorptions (cf. schemes 4 and 5). The SH-MCM-41 adsorbent remained selective to gold adsorption even at the elevated pH and high organic content found in the electroplating waste solution (Fig. 6b).

4.2. Adsorption modeling

The grafting of thiolpropyl and aminopropyl groups onto MCM-41 introduces surface heterogeneity, and therefore Freundlich adsorption model (i.e., $q_e = KC_e^n$) was used to model adsorption on the NH_2-MCM-41 and SH-MCM-41. Fig. 1a and b show that Freundlich equation fits the gold adsorption data well. The corresponding sums of square error (SSE) are 0.016 and 0.020, respectively. The LeVan and Vermeulen model [31], derived from the ideal adsorption solution (IAS) theory of Myers and Prausnitz [39], was used to predict the binary adsorptions from the single component adsorption data. The effects of anion were taken into account using the published data on dissociation constant of the metal salts. It is clear that there is a good agreement between the model and experiment (cf. Figs. 1c and d and 2c and d). Gold adsorption on thiolpropyls is insensitive to anions according to the adsorption scheme 3b in Fig. 8b, however gold complexation on

aminopropyls (Fig. 8a, scheme 2) involves dissociation and anions in the solution are expected to have a strong effect. According to the model, the lower gold adsorption capacity of NH_2-MCM-41(b) for the binary adsorption (i.e., 1.05 mmol/g) compared to single component adsorption capacity of 1.4 mmol/g is due to the higher concentration of anions in the binary solution. No attempt was made to model gold adsorption from the multi-components systems (i.e., simulated gold mining solution and gold electroplating waste) because of their complexity.

Experiments and model suggest that pH and anion content of the eluent are important parameters for the recovery of adsorbed gold. This observation enabled us to design a new eluent based on acidified saline solution, thus minimizing the use of caustic acids. The choice of eluents is important for the recovery and regeneration of the MCM-41 adsorbents. Alkaline eluents that could dissolve and damage the siliceous MCM-41 must be avoided, along with chemicals that react or form strong complexes with the grafted functional groups (e.g., thiolpropyl and aminopropyl). Mineral acids are among the common eluents used, in addition to EDTA, sodium thiosulphate and thiourea. Feng et al. [20] successfully recovered mercury from thiolpropyl grafted MCM-41 using a strong hydrochloric acid solution. They also reported that the acid-regenerated adsorbent was reusable. However, this study showed that gold adsorbed on SH-MCM-41 is difficult to recover even with 5 M HCl solution (Table 3). The addition of sodium chloride salt to increase the anion concentration was also ineffective. This indicates that gold was strongly adsorbed on the thiolpropyl groups. It is possible to recover the adsorbed gold using thiosulfate at a neutral pH, but the process was slow and further studies must be carried out.

5. Concluding remarks

This work shows that mesoporous MCM-41 containing grafted aminopropyl and thiolpropyl groups are selective for gold adsorption. The adsorption mechanisms are different. The gold adsorption on NH_2-MCM-41 at low pH was between the positively charged $–RNH_3^+$ and the negatively charged $AuCl_4^-$ anion. The protonated amino groups ($–RNH_3^+$) was a Lewis acid and repelled the positively charged cations (e.g., Cu^{2+}, Ni^{2+}, Fe^{3+}) and prevented their adsorptions. This resulted in the excellent adsorption selectivity of NH_2-MCM-41 at low pH for both binary and complex mixtures containing gold. However, the $–RNH_3^+$ also adsorbed other anions such as $PdCl_4^{2-}$ from the mining solution. The NH_2-MCM-41 was sensitive to pH and adsorbed metal cations above $pH_{p.z.c.}$ resulting in poor selectivity. The SH-MCM-41 was insensitive to pH and adsorbed only gold. The $AuCl_4^-$ anions were adsorbed as $–RSAuCl_3^-$ complex. The SH-MCM-41 is the more efficient adsorbent with each thiolpropyl adsorbing one gold atom, while two aminopropyls in NH_2-MCM-41 were needed to adsorb one gold atom. Gold was readily recovered as high purity gold chloride solutions (> 90%) by elution with an acid (i.e., 5 M HCl) or an acidified saline solution (i.e., 1 M HCl + 4 M NaCl) from spent NH_2-MCM-41. The gold recovery from SH-MCM-41 was more difficult and required the use of thiolsulfate instead of acid solutions. The regenerated adsorbents exhibited the same adsorption capacity and selectivity as the fresh adsorbent.

Acknowledgements

The authors gratefully acknowledge the funding from the Hong Kong Research Grant Councils (grant RGC-HKUST 6037/00P) and the Environment & Conservation Fund (ECWW05/06.EG01). We thank the Material Characterization and Preparation Facility at the HKUST for the use of XRD, SEM, TEM, XPS and TGA/DTA equipment and the Advanced Engineering Material Facility for the use of Coulter SA3100 surface area and pore size analyzer and Beckman Coulter Zeta-Potential analyzer.

References

[1] D.S. Cameron, Fuel cells—science and technology 2004, Platinum Met. Rev. 49 (2005) 16–20.
[2] K.L. Yeung, E.E. Wolf, J. Catal, STM studies of size and morphology of Pt graphite catalysts, J. Catal. 135 (1992) 13–26.
[3] K.L. Yeung, J.M. Sebastian, A. Varma, Novel preparation of Pd/Vycor composite membranes, Catal. Today 25 (1995) 231–236.
[4] K.L. Yeung, R. Aravind, J. Szegner, A. Varma, Metal composite membranes: synthesis, characterization and reaction studies, Stud. Surf. Sci. Catal. 101 (1996) 1349–1358.
[5] P. Goodman, Current and future uses of gold in electronics, Gold Bull. 35 (2002) 21–26.
[6] S.P. Fricker, Medical uses of gold compounds: past, present and future, Gold Bull. 29 (1996) 53–60.
[7] M. Haruta, Gold as a novel catalyst in the 21st century: preparation, working mechanism and applications, Gold Bull. 37 (2004) 27–36.
[8] K.Y. Ho, K.L. Yeung, Effects of ozone pre-treatment on the performance of Au/TiO_2 catalyst for CO oxidation reaction, J. Catal. 242 (2006) 131–141.
[9] Electronics Industry Environmental Roadmap, Microelectronics and Computer Technology Corporation (MCC), Austin, TX, 1996.
[10] M. Meltzer, M. Callahan, T. Jensen, Metal-bearing Waste Streams: Minimizing, Recycling and Treatment, Noyes Data Corp., Park Ridge, NJ, 1990.
[11] W. Petruk, Applied Mineralogy in the Mining Industry, Elsevier Science, New York, 2000.
[12] J. Cui, E. Forssberg, Mechanical recycling of waste electric and electronic equipment: a review, J. Hazard. Mater. 99 (2003) 243–263.
[13] N.H. Chung, M. Tabata, Selective extraction of gold(III) in the presence of Pd(II) and Pt(IV) by salting-out of the mixture of 2-propanol and water, Talanta 58 (2002) 927–933.
[14] W.J. Thomas, B.D. Crittenden, Adsorption Technology and Design, Butterworth-Hienemann, Oxford, 1998.
[15] K.L. Rees, J.S.J. van Deventer, The mechanism of enhanced gold extraction from ores in the presence of activated carbon, Hydrometallurgy 58 (2000) 151–167.
[16] P.K. Jal, S. Patel, B.K. Mishra, Chemical modification of silica surface by immobilization of functional groups for extractive concentration of metal ions, Talanta 62 (2004) 1005–1028.
[17] R. Celis, M.C. Hermosin, J. Cornejo, Heavy metal adsorption by functionalized clays, Env. Sci. Technol. 34 (2000) 4593–4599.
[18] A. Dabrowski, Z. Hubicki, P. Podkoscielny, E. Robens, Selective removal of the heavy metal ions from waters and industrial wastewaters by ion-exchange method, Chemosphere 56 (2004) 91–106.
[19] I.M.N. Vold, K.M. Vårum, E. Guibal, O. Smidsrød, Binding of ions to chitosan—selectivity studies, Carbohydr. Polym. 54 (4) (2003) 471–477.
[20] X. Feng, G.E. Fryxell, L.-Q. Wang, A.Y. Kim, J. Liu, K.M. Kemner, Functionalized momolayers on ordered mesoporous supports, Science 276 (1997) 923–926.
[21] O. Olkhovyk, V. Antochshuk, M. Jaroniec, Benzoylthiourea-modified MCM-41 mesoporous silica for mercury(II) adsorption from aqueous solutions, Colloids Surf. A: Physicochem. Eng. Aspects 236 (2004) 69–72.
[22] J. Aguado, J.M. Arsuaga, A. Arencibia, Adsorption of aqueous mercury(II) on propylthiol-functionalized mesoporous silica obtained by cocondensation, Ind. Eng. Chem. Res. 44 (10) (2005) 3665–3671.
[23] J. Brown, L. Mercier, T.J. Pinnavaia, Selective adsorption of Hg^{2+} by thiol-functionalized nanoporous silica, Chem. Commun. (1999) 69–70.
[24] T. Kang, Y. Park, K. Choi, J.S. Lee, L. Yi, Ordered mesoporous silica (SBA-15) derivatized with imidazole-containing functionalities as a selective adsorbent of precious metal ions, J. Mater. Chem. 14 (2004) 1043–1049.
[25] K.F. Lam, K.L. Yeung, G. McKay, A rational approach in the design of selective mesoporous adsorbents, Langmuir 22 (2006) 9632–9641.
[26] K.F. Lam, K.L. Yeung, G. McKay, An investigation of gold adsorption from a binary mixture with selective mesoporous silica adsorbents, J. Phys. Chem. B 110 (2006) 2187–2194.
[27] K.F. Lam, K.L. Yeung, G. McKay, Preparation of selective mesoporous adsorbents for $Cr_2O_7^{2-}$ and Cu^{2+} separation, Microporous Mesoporous Mater. 100 (2007) 191–201.
[28] K.F. Lam, K.L. Yeung, G. McKay, A new approach for Cd^{2+} and Ni^{2+} removal and recovery using mesoporous adsorbent with tunable selectivity, Env. Sci. Technol. 41 (2007) 3329–3334.
[29] K.F. Lam, K.Y. Ho, K.L. Yeung, G. McKay, Selective adsorbents from chemically modified ordered mesoporous silica, Stud. Surf. Sci. Catal. 154C (2004) 2981–2986.
[30] K.Y. Ho, G. McKay, K.L. Yeung, Selective adsorbents from ordered mesoporous silica, Langmuir 19 (2003) 3019–3024.
[31] M.D. LeVan, T. Vermeulen, Binary Langmuir and Freundlich isotherms for ideal adsorbed solutions, J. Phys. Chem. 85 (1981) 3247–3250.
[32] M. Kruk, M. Jaroniec, A. Sayari, Relations between pore structure parameters and their implications for characterization of MCM-41 using gas adsorption and X-ray diffraction, Chem. Mater. 11 (1999) 492–500.

[33] D.G. Castner, K. Hinds, D.W. Grainger, X-ray photoelectron spectroscopy sulphur 2—study of organic thiol and disulfide binding interactions with gold surfaces, Langmuir 12 (1996) 5083–5086.
[34] A.E. Martell, R.M. Smith, Critical Stability Constants, Plenum Press, New York, 1974.
[35] P.J. Murphy, M.S. Lagrange, Raman spectroscopy of gold chloro-hydroxy speciation in fluids at ambient temperature and pressure: a re-evaluation of the effects of pH and chloride concentration, Geochim. Cosmochim. Acta 62 (1998) 3515–3526.
[36] K.F. Lam, C.M. Fong, K.L. Yeung, Separation of precious metals using selective mesoporous adsorbents, Gold Bull. 40 (3) (2007) 192–198.
[37] R.G. Pearson, Chemical hardness and bond dissociation energies, J. Am. Chem. Soc. 110 (1988) 7684–7690.
[38] A. Trokhimchuk, E.B. Andrianova, V.N. Losev, Interaction peculiarities of gold(III) with silica gels containing both aminopropyl and mercaptopropyl surface groups, Adsorp. Sci. Technol. 22 (10) (2004) 837–848.
[39] A.L. Myers, J.M. Prausnitz, Thermodynamics of mixed-gas adsorption, AIChE J. 11 (1) (1965) 121–127.